

Neha Dixit, N.V.Kartheek M and Jayanthi Sivaswamy

Abstract- We propose a method for synthetic zooming of tomographic images by applying super resolution technique on reconstructed data via a combination of rotated lattices (CRL). The proposed method consists of 2 steps: (i) Sinogram data is filtered and backprojected on to two lattices, which are rotated versions of each other and (ii) the samples from the two lattices are interpolated to find the upsampled image. Square and hexagonal lattices have been investigated for CRL. Results of subjective and objective evaluations of the proposed method on analytic phantoms are presented and compared with direct upsampling of data reconstructed on a single square lattice. The proposed method shows qualitative and quantitative improvement over direct upsampling in general with the combination of hexagonal lattices yielding better results than square lattices.

I. INTRODUCTION

Improving resolution of tomographic images has been an active area of research in the past few years. Super resolution (SR) techniques based on combination of a set of low resolution images with spatial shifts have been examined for PET [3][4] and CT [2] images. Improving the resolution of a region of interest via synthetic zooming or upsampling is also of interest in medical imaging for a variety of reasons.

In this paper, we present a method for this task where we apply the concept of SR to obtain up-sampled images of superior quality. In general, the concept of super resolution relies on using a combination of low resolution images which provide a ‘different view’ of a scene. While the methods in [2-4] have only focused on views which are related by sub-pixel shifts, we examine a different alternative: the views are related by a rotation. For simplicity, the remaining part of this paper will assume parallel beam tomography and reconstruction by filtered back projection.

II. METHOD

Let $I(x,y)$ be the imaged object and $P(r,\theta)$ be the corresponding sinogram data where (r,θ) are both discrete. The process of reconstruction as described in [4] consists of two main steps: *back-projection* of $P(r,\theta)$ into a continuous image $I_R(x,y)$ and *sampling* of $I_R(x,y)$ to generate a digital image $I_R[n_1,n_2]$ where $[n_1,n_2]$ are discrete. Assuming the image $I_R[n_1,n_2]$ is of size $M \times M$, in order to up-sample this image by a factor of k , the traditional approach is to introduce $(k-1)$ zeros row- and column-wise and interpolate between the non-zero valued samples. The limitation with this approach is that the result entirely depends on the choice of the interpolation kernel as no new data has actually been used to derive the required new samples. Alternatively, one could generate two non-overlapping sets of samples from $I_R(x,y)$ and then interpolate between these samples. Union of shifted lattices is one option [1]. We propose a different option, namely to generate these two sets by sampling with 2 lattices which are

rotated versions of each other: Consider 2×2 sampling matrices V and $V_\phi = T_\phi V$, where T_ϕ is a rotation matrix. The desired sets of samples I_R and $I_{R\phi}$ are then given as $I_R[n] = I_R(Vn)$ and $I_{R\phi}[n] = I_R(V_\phi n)$ where $n = [n_1, n_2]^T$. The samples obtained by combining the samples from I_R and $I_{R\phi}$ are shown in Figure (1a) for $\phi = 45^\circ$. In the preceding formulation, the matrix V will vary with the choice of sampling lattice, namely square or hexagonal. Hexagonal lattices offer superior packing efficiency with non-orthogonal bases [5][6] and hence are included. The sample points derived from a combination of hexagonal lattices are shown in Figure (1b) for $\phi = 30^\circ$. The desired upsampled image I_R^k is found as $(I_R + I_{R\phi}) * h_i$, where $*$ denotes convolution and h_i is an interpolating function. In the following, S^k denotes result of upsampling applied directly to $I_R[n]$. The upsampled (by k) result is denoted S_c^k (H_c^k) which is obtained from combination of samples from the square (hexagonal) and rotated square (hexagonal) lattices.

III. Experiments and Results

We have implemented the above method as follows: thin plate splines were chosen for interpolation, ϕ was taken to be 45° and 30° for square and hexagonal lattices, respectively, to minimize overlap between I_R and $I_{R\phi}$ sample points. Hexagonal lattice with basis vectors $(1,0)$ $(1/\sqrt{3},1)$ and $(1,1/\sqrt{3})$, $(0,1)$ was used to generate a good distribution of samples. Up-sampling factors of $k = 2, 4$ and 6 were tested. In all cases, the final image I_R^k was computed on a square lattice.

Three analytic phantoms were designed to generate the sinograms (varying in size from 101×180 to 211×180) used in our experiments: *Rings* (concentric circles with spacing inversely proportional to the radii) to study preservation of curved structure; *Lines* to study the effect on lines at different angular orientation and *Dots* to compare the contrast and spatial resolution of the up-sampled image. The upsampled images of the phantoms were evaluated qualitatively and quantitatively by comparing S^k , S_c^k and H_c^k .

The qualitative results of upsampling for the 3 phantoms are shown in Figure 2(a-c), Fig. 3 and Fig. 4. These results show that the combination of lattices does improve the quality over a single lattice in the case of *Rings* and *Lines*. The rings are crisper in S_c^4 and H_c^4 compared to S^4 and the central region of *Lines* is best defined in the case of H_c^2 .

Quantitative evaluation using the IQM toolbox [7] and line profile plot is presented for the *Rings* and *Dots*. The energy distribution, computed from the normalized power spectrum of an image, in angular (-90° to 90° in steps of 4°) direction is shown in Fig. 2(d) and radial ρ (64 bands) direction is shown in Fig. 2(e). On average, there is a boost in the energy for all angles over S^4 with a directional bias evident at $\pm 45^\circ$ for S_c^4 .

The energy variation across ρ is seen to be much smoother for S^4_c and H^4_c compared to S^4 due to reduction in imaging. Despite a similarity in visual quality of the *Dots* in Fig 4 (a-c), there is a boost in contrast as seen in Table 1 which lists C values for the sixth row of *Dots*. C was computed as (P-T)/P where P and T are peak and trough values. The boost in contrast is mainly due to the lower T values as seen in the corresponding line profiles in Fig. 4(d).

	1	2	3	4	5	6	7
S^2	0.672	0.692	0.663	0.655	0.663	0.692	0.672
S^2_c	0.738	0.759	0.750	0.745	0.750	0.759	0.738
H^2_c	0.761	0.764	0.739	0.741	0.737	0.758	0.761

Table 1. Contrast values of the sixth row of dots in Fig. 4 (a-c)

IV. CONCLUSIONS

Upsampling of a reconstructed images using combination of lattices produces visually and quantitatively improved results over direct upsampling. This is an alternative way of applying SR technique to improving the resolution of tomographic images. Current investigations are on noisy data and scanner-sourced data.

V. REFERENCES

- 1) H. Behmard, "Reconstruction of 2-D signals from union of shifted lattices", Proc. ICASSP, vol(4), 197-200, 2005.
- 2) S.H.Izen, D.P.Rohrer and K.L.A. Sastry, "Exploiting symmetry in fan beam CT: Overcoming third generation undersampling" SIAM J. Appl Math, 65(3):1027-1052, 2005.
- 3) J. A. Kennedy, O. Israel, A. Frenkel, R. Bar-Shalom, and H. Azhari, "Super-resolution in PET imaging", IEEE Trans Medical Imaging 25(2), 137-147, 2006.
- 4) G Chang, T Pan, J Clark, Jr, OR Mawlawi, "Comparison between two super-resolution implementations in PET imaging" Med. Phys. 36 (4) 2009.
- 5) A. Yabushita, "Image reconstruction with hexagonal grid" Med Imaging technology 21(3), 239-245(2003).
- 6) M. Knaup, S.Steckmann, O.Bockenbach, M. Kachelrieß, "CT image reconstruction using hexagonal grid", Nuclear science symposium, Vol 4, 3074-3076,(2007).
- 7) N.B. Nill and B.H. Bouzas, "Objective Image Quality Measure Derived from Digital Image Power Spectra", Optical Engineering, vol.31, pp.813-825, April 1992.

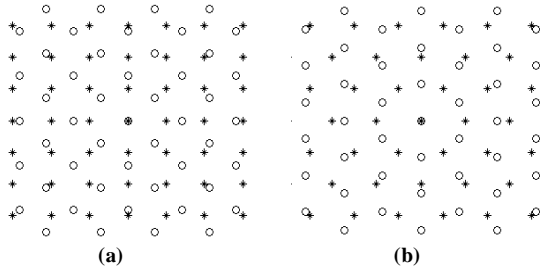
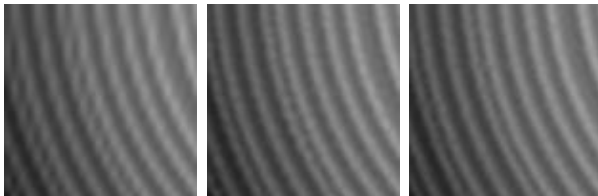


Fig.1. Sample points drawn from a combination of lattices: (a) S (*) and S_{45} (o) and (b) H (*) and H_{30} (o).



(a) S^4 (b) S^4_c (c) H^4_c
Fig.2. Upsampled (by 4) ROIs of concentric rings.

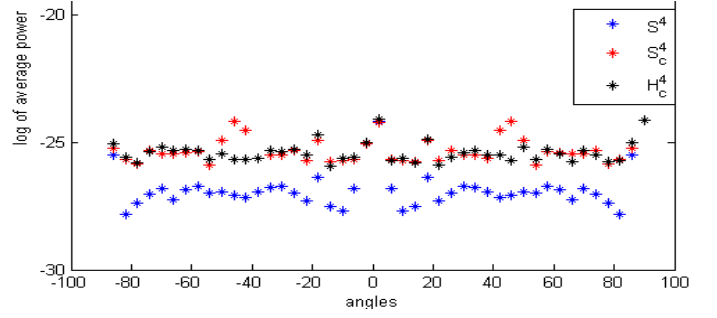


Fig. 2(d). Normalised energy distribution across orientation bands for *Rings*.

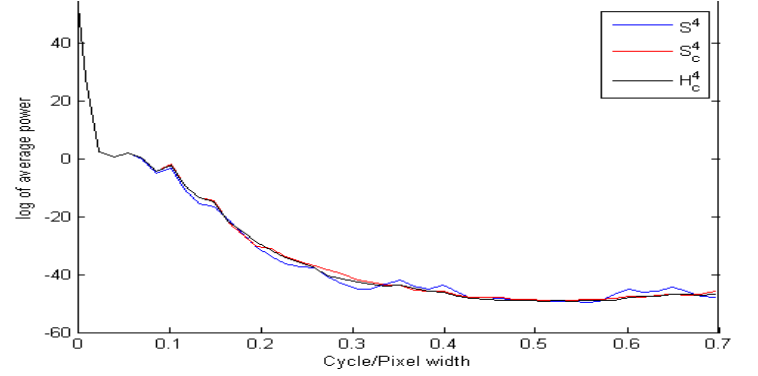


Fig. 2(e). Normalised energy distribution across radial bands for *Rings*.

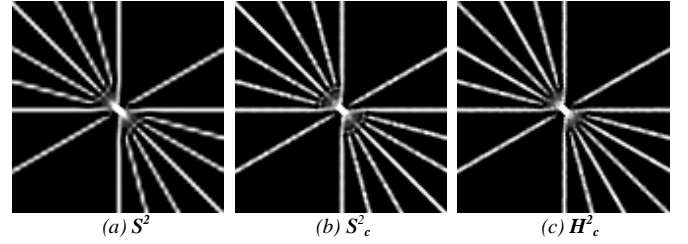


Fig. 3. Results of upsampling *Lines*. Only a region is shown.

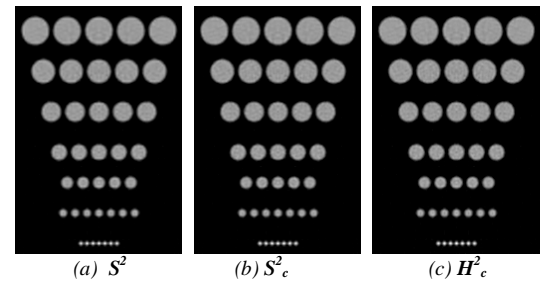


Fig. 4 (a), (b) and (c). Results of upsampling *Dots*.

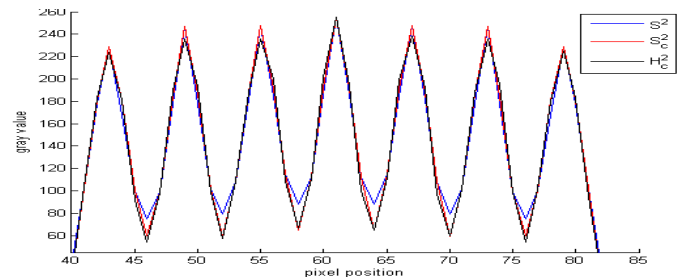


Fig. 4 (d). The line profile of the sixth row of dots in (a), (b) and (c).